HHS Public Access

Author manuscript

Neurogastroenterol Motil. Author manuscript; available in PMC 2020 March 01.

Published in final edited form as:

Neurogastroenterol Motil. 2019 March ; 31(3): e13484. doi:10.1111/nmo.13484.

Necrotizing enterocolitis attenuates developmental heart rate variability increases in newborn rats

Alissa L. Meister[1], **Kim K. Doheny**[1,2], and **R. Alberto Travagli**[1]

[1]Neural and Behavioral Sciences, Penn State College of Medicine, Hershey PA

[2]Neonatal-Perinatal Medicine, Penn State College of Medicine, Hershey PA

Abstract

Background: We have shown previously that a decreased high frequency spectrum of heart rate variability (HF-HRV), indicative of reduced vagal tone, shows promise in predicting neonates likely to develop necrotizing enterocolitis (NEC) before its clinical onset. We hypothesized that NEC induction in rat pups decreases HF-HRV power; subdiaphragmatic vagotomy worsens the severity of the NEC phenotype, increases levels of pro-inflammatory cytokines, and alters the myenteric phenotype.

Methods: Newborn Sprague-Dawley rats, representative of preterm human neonates, were subjected to 7–8 days of brief periods of cold stress and hypoxia to induce NEC with or without unilateral subdiaphragmatic vagotomy. HRV was measured at postnatal days one and five, pups were sacrificed at day 8/9, gastrointestinal tissues and blood were collected for immunohistochemical, corticosterone, and cytokine analysis.

Key Results: Compared to control, NEC-induced rats showed: i) typical histological signs of grade 2 NEC, which were more severe in rats that underwent vagotomy; ii) reduced developmental increases in time (RMSSD) and frequency (HF) HRV spectra when combined with the stress of laparotomy/vagotomy; iii) increases in nitric oxide synthase-immunoreactivity in the myenteric plexus of jejunum and ileum; furthermore, compared to mild NEC and controls, vagotomized NEC rats had increased plasma values of pro-inflammatory cytokines IL-1β and IL-6.

Conclusions & Inferences: Our data suggest that in rodents, similar to neonatal observations, NEC induction attenuated developmental HF-HRV increases, furthermore, subdiaphragmatic vagotomy worsened the histological severity, increased pro-inflammatory cytokines, and altered the nitrergic myenteric phenotype, suggesting a role of the vagus in the development of NEC pathology.

Keywords

HF power; immunohistochemistry; nNOS; pro-inflammatory cytokines; vagus

*Corresponding author: Dr. R. Alberto Travagli, Department of Neural and Behavioral Sciences, Penn State College of Medicine, 500 University Drive, MC H109, Hershey, PA 17033, rtravagli@pennstatehealth.psu.edu.

Competing Interests: the authors have no competing interests.

In the United States ~10% of neonates are born at a gestational age less than 37 weeks[1], of these neonates, those born at a very-low birth weight (VLBW; <1,500g) are at an increased risk for morbidities, including necrotizing enterocolitis (NEC). Approximately 5–12% of VLBW neonates develop NEC, with a higher incidence in more crowded and stressful neonatal intensive care units (NICU), and approximately 30% of these patients will not survive[2–6].

In rodent models, histological NEC is characterized by damage to the intestinal wall ranging from mild mucosal injury in the early phases of the disease (grade 1–2), to pneumatosis intestinalis, submucosal hemorrhage, and perforation as the disease progresses to fulminant NEC with intestinal necrosis (grade 3–4)[7]. In humans, risk factors for NEC include preterm birth, VLBW, formula feeding, mechanical ventilation, and infections such as chorioamnionitis[6,8,9]. The subtle and often fast onset of NEC mandates the development of minimally invasive predictive methods to identify neonates at risk before they develop clinical NEC[6,8,9]. Likewise, it is necessary to develop animal models that mimic the early stages of NEC when such predictive tests would allow the development of disease-modifying treatments or preventative therapies to be employed.

The high-frequency (HF) spectrum of heart rate variability (HRV) is a non-invasive way to measure vagal tone indirectly in neonates, and previous studies have identified HRV as a marker for fetal and neonatal well being[10–13]. HRV measures can be calculated based on electrocardiogram (ECG) recordings, using a fast Fourier transformation of inter-beat-interval (IBI) values for both time- and frequency-domain analysis[11,12,14–18]. In time-domain analysis, the difference between sequential IBI values and root-mean-square of successive differences (RMSSD) represent vagal tone, similarly, the HF power spectrum in frequency-domain analysis assesses indirectly vagal parasympathetic outflow, which modulates the functions of the upper gastrointestinal (GI) tract from the lower esophagus to the transverse colon through the dorsal motor nucleus of the vagus (DMV)[11,12,14–19].Conversely, the low frequency (LF) spectrum of HRV frequency-domain analysis represents a mix of sympathetic and parasympathetic outflow[11,12,14–18].

Initial clinical observations reported altered heart rate characteristics and variability in fetuses and premature infants with chorioamnionitis or NEC[20–22]. Since then, our group has shown that preterm neonates, who later develop NEC, display a diminished HF-HRV power prior to the onset of clinical signs, as compared to healthy controls that display significantly higher HF-HRV power throughout the study[10]. Therefore, we proposed that a decrease in HF-HRV power is a promising method to predict which neonate is at risk of developing NEC. Such predictive tests, however, have not been assessed in a preclinical rodent model in the laboratory setting.

The aims of the present study were to test the hypotheses that an attenuated, established NEC induction model will i) decrease HF-HRV power, ii) alter selectively the myenteric neurochemical phenotype of the distal small intestine; that pups with attenuated NEC and subdiaphragmatic vagotomy will show iii) worsened severity of the histopathological NEC phenotype, and iv) increased levels of systemic plasma pro-inflammatory cytokines.

MATERIALS AND METHODS

Ten pregnant (embryonic day 13) Sprague-Dawley dams were housed in an AAALAC accredited Animal Care Facility maintained at 24°C on a 12:12 hour light:dark cycle with food and water provided ad libitum. Upon birth, pups were randomly separated into the following groups: i) control; ii) control+sham vagotomy; iii) control+vagotomy; iv) mild NEC (i.e. grade 2 or lower); v) mild NEC+sham vagotomy; vi) mild NEC+vagotomy; and, vii) full NEC (i.e. grade 3 or higher). Previous studies relating human development, particularly neural development, have shown that rats at postnatal day 12/13 represent a term human neonate; therefore newborn rat pups are an excellent model for the study of preterm neonates[23–25].

All procedures outlined below were performed using aseptic techniques and were conducted in accordance with NIH guidelines, with the approval of the Penn State University College of Medicine Institutional Animal Care and Use Committee, and according to the journal policies and regulations on animal experimentation.

NEC Induction and Surgery

Starting at postnatal day (P) 2, pups in the mild NEC groups were exposed to hypoxia (breathing 92/8% N_2/O_2 for 10 min) and cold stress (4°C for 10 min) twice daily[7,26,27], an accepted model, albeit not without controversy[28]. Pups in both control+vagotomy and mild NEC+vagotomy groups underwent a subdiaphragmatic unilateral vagotomy[29] prior to the first exposure to hypoxia and cold stress, on P1. Briefly, pups were anesthetized with isofluorane (3% in air; Vedco, Saint Joseph, MO, USA), and an abdominal laparotomy was performed to expose the anterior subdiaphragmatic vagus nerve along the esophagus. Using microscopic guidance, the anterior gastric branch was identified and sectioned, and the incision was closed with 8–0 thread before pups were allowed to recover in an incubator at 37.5° C. At P5 pups were injected intraperitoneally with 100μl Fluorogold® (0.5mg ml^{-1} in sterile saline; Fluorochrome, Denver, CO, USA) to label GI-projecting DMV neurons and, at the end of the experiment, confirm the efficacy of vagotomy using brainstem slices with a Nikon E-400 microscope equipped with ultraviolet filters (Nikon, Tokyo, Japan). Pups with an incomplete anterior subdiaphragmatic vagotomy were transferred to the sham group a posteriori. Control+sham and mild NEC+sham pups received an abdominal laparotomy and gastro-esophageal manipulation prior to the first exposure to hypoxia and cold stress, but the subdiaphragmatic vagus nerve was left untouched. See Figure 1 for a schematic showing the experimental design.

To induce full NEC, pups were separated from dam at time of birth, prior to suckling. Pups were maintained individually in an Ohio® IC Incubator at 37.5°C (Ohio®Medical, Gurnee, IL, USA), underwent asphyxia and cold stress twice daily, and received 100μl of hypertonic formula feeding (0.2g Similac®PM, Abbott, Chicago, IL, USA, mixed with 0.19g Esbilac, PetAg, Hampshire, IL, USA, in 1mL warm water) every 3–4 hours for the first 48 hours of life, then every 6 hours until death.

Heart rate variability measures

Pups were weighed daily between 8–9 a.m. Five-ten minutes recordings with a bilateral two lead electrocardiogram (ECG; sampling rate 1000Hz) were taken at P1, i.e. baseline values before disease induction, and at P5 to quantify HRV changes that may be occurring during the early phases of NEC. All ECG recordings were performed at a standardized time, i.e. after early morning nursing between 6–9 a.m., in all but full NEC groups due to the fact that at the same time points NEC rats had already undergone ~12 hours of maternal separation and could not be compared with other groups. Each HF-HRV power data point was the average of at least four 60s non-overlapping segments conducted during a 5–10min-long recording acquired with Axoscope® 10.3 software (Molecular Devices, Sunnyvale, CA, USA) and imported into MiniAnalysis® 6.0.7 (Synaptosoft, Fort Lee, NJ, USA), to isolate the peak of each R wave during the ECG recordings. The IBI difference values were then analyzed using HRV Analysis Software (HRVAS, available at https://github.com/jramshur/HRVAS) in preselected 60s-long segments containing minimal noise and movement[30]. Based on data in literature, the HF bandwidth was set at 1–3Hz[31,32]. RMSSD was calculated with the following formula:

$$RMSSD = \sqrt{\frac{\int_{i=1}^{N-1} \left((R-R)_{i+1} - (R-R)_i\right)^2}{N-1}}$$

Where R is the time of the peak of the R wave and N is the total number of R waves measured in each trace[14].

Histology and Immunohistochemistry

At P8/9, pups were anesthetized with isoflurane (3% in air; Vedco Inc., St. Joseph, MO), a cardiac puncture was performed to obtain 200μl blood, then pups were perfused with saline followed by 4% paraformaldehyde (PFA) in phosphate buffer (PBS), and the entire GI tract was extracted.

Samples of the gastric corpus and fundus, duodenum, jejunum, and ileum were fixed in 10% neutral-buffered formalin for 24 hours before being processed using a Shandon Citadel 1000 (Thermo Fisher Scientific, Waltham, MA, USA). After processing, samples were embedded in paraffin and sliced into 6μm–thick sections. Samples were then de-paraffinized and rehydrated, stained with hematoxylin-eosin, dehydrated, and covered with Cytoseal™60 (Thermo Fisher Scientific). An observer blinded to groups scored tissues for histological NEC severity based on the presence of i) intact morphology (Grade 0, control), ii) sloughing of epithelial cells at the tips of the villi (Grade 1, mild NEC), iii) mid-villous necrosis (Grade 2, NEC), iv) loss of villi or complete villous necrosis (Grade 3, NEC), and v) complete destruction of the mucosa, transmural necrosis, and pneumatosis intestinalis (Grade 4, NEC)[33].

The remaining portions of the extracted GI tract, including the gastric corpus and fundus, duodenum, jejunum, and ileum, were stretched with dissection pins on a wax-covered petri

dish, and fixed with 4% PFA in PBS for 12–24 hours, then longitudinal muscle-myenteric plexus preparations were dissected and reacted for immunohistochemistry of the myenteric plexus, as described previously[34]. Briefly, tissue samples were rinsed in PBS and Tris-buffered PBS (TPBS) containing 0.3% Triton X-100 (Millipore, Burlington, MA, USA) and 0.05% thimerosal (Sigma-Aldrich, St. Louis, MO, USA), blocked with 10% normal horse serum (NHS; Thermo Fisher Scientific), then incubated for four-five days at room temperature on a shaker with rabbit α-protein gene product 9.5 (1:500; PGP; Millipore) and either goat α-neuronal nitric oxide synthase (1:1,000; nNOS; Abcam, Cambridge, United Kingdom) or goat α-choline acetyl transferase (1:200; ChAT; Millipore) to quantify the proportion of postganglionic myenteric neurons of the non-adrenergic non-cholinergic or the cholinergic pathway, respectively. Samples were then rinsed and incubated overnight with the following secondary antibodies: Alexa Fluor 488 donkey α-goat (1:1000; Life Technologies, Eugene, OR, USA) and Alexa Fluor 568 donkey α-rabbit (1:1000; Life Technologies).

Immunofluorescent images were captured with an Olympus Fluoview FV1000 confocal laser-scanning microscope with the FV10-ASV 4.2 viewer software (Olympus, Shinjuku, Tokyo, Japan). The FV10-ASV 4.2 viewer software was also used to count the number of cells stained positive for nNOS, ChAT, and PGP. PGP was used in all samples to quantify the total number of cells; a minimum of 100 PGP-positive neurons was counted in each sample to obtain the percentage of ChAT or nNOS positive myenteric neurons.

Corticosterone and Cytokine Quantification

At sacrifice, blood was collected via cardiac puncture immediately (within 3 minutes) after the animal was anesthetized with isoflurane, and stored in a Microtainer™ (BD, Franklin Lakes, NJ, USA) with EDTA at −20°C. Before analysis, blood was briefly allowed to thaw on ice before being separated using a Centrifuge 5417R (11900rpm, 4°C, 10 minutes; Eppendorf, Hamburg, Germany) prior to plasma corticosterone and cytokine analysis.

Fifty-five plasma samples were run in duplicate using the Enzo Corticosterone ELISA Kit (Farmingdale, NY, USA) according to manufacturer instructions at 1:40 dilution (sensitivity reported as 26.99 pg ml^{-1}). The optical density (405nm) of the samples was measured using a Spectramax Gemini plate reader (Molecular Devices, Sunnyvale, CA, USA) interfaced with Softmax® Pro 6.3.1 software (Molecular Devices). The calibrator concentration curve was calculated using an online freely-available immunoassay software package utilizing a 4 parameter logistic curve fitting program (https://www.myassays.com), and unknown concentrations were determined via interpolation.

To quantify plasma levels of IFN-γ, IL-1β, IL-6, IL-10, and TNF-α, 53 samples were assayed in duplicate using the MSD® V-Plex Custom Pro-inflammatory Panel 2 (Rat) kit (Meso Scale Discovery®, Rockville, MD, USA) according to manufacturer specifications at 1:32 dilution. The lower and upper limits of quantification were (in pg ml^{-1}) 39.7–3,750 for IFN-γ, 102–8,100 for IL-1β, 96.9–8,550 for IL-6, 163–15,700 for IL-10, and 9.10–793 for TNF-α. Assays were read using a MESO QuickPlex SQ 120 and analyzed using DISCOVERY WORKBENCH 4.0 (Meso Scale Discovery®).

Statistical Analysis

All data were analyzed using SPSS version 24 (IBM Corporation, Armonk, NY). For HRV data, within-group between-time point data were analyzed using repeated-measures ANOVA. Between groups differences at the same time point were analyzed using one-way ANOVA followed by a post-hoc Bonferroni Procedure. All other between group data, including blood assays and immunohistochemistry, were analyzed using one-way ANOVAs, to compare groups in the same tissue type or cytokine. Significance was set at $p<0.05$.

RESULTS

Vagotomy increases the histological score of NEC severity.

Gross anatomy and histology of specimens from the duodenum, jejunum, and ileum of the different groups showed undamaged villi in control (n=12 pups), control+sham (n=10 pups) and control+vagotomy (n=6) groups, sloughing of epithelial cells at the tips of the villi in mild NEC (n=16 pups) and mild NEC+sham (n=9 pups) groups (grade 1 NEC). An increased severity of NEC, including mid-villous necrosis (grade 2 NEC), was observed in the mild NEC+vagotomy (n=11 pups) group. In 5 pups which received the full NEC induction, the severity of NEC was increased to include the complete destruction of the mucosa, transmural necrosis, pneumatosis intestinalis, and intramural hemorrhage (grade 4 NEC; Figure 2). The full NEC group was not included in further analysis due to the high mortality rate of the pups, 80% died within 72 hours of birth and all died within 5 days. No pups died as a consequence of mild NEC induction, while 33.3% of control+sham, 14% control+vagotomy, 42% of mild NEC+sham surgery, and 50% of mild NEC+vagotomy pups were killed by their dam after surgery.

These data indicate that vagotomy worsened the histopathological profile of pups which received mild NEC induction, and that vagal dysfunction plays a role in the onset or worsening of NEC.

NEC attenuates developmental HRV increases.

At P1, i.e. before the start of any NEC induction, all rats displayed similar heart rates ($p>0.05$ for all groups vs control), with a significant increase in all groups at P5 ($p<0.05$ vs. P1 for all groups; $p>0.05$ vs. control for all groups); this time point represents the early phases of the disease process, when human neonates would be targeted for preventative care. Data are summarized in Table 1.

At P1 similar HF-HRV power, LF-HRV power and RMSSD levels were observed in all the groups ($p>0.05$ for all groups vs control). At P5, control (N=12), control+sham (N=10), and mild NEC (N=16) pups displayed similar increases in HF-HRV power, LF-HRV power, and RMSSD ($p<0.05$ vs P1 for all groups; $p>0.05$ vs control at P5). Conversely, no significant increase in HF-HRV power, LF-HRV power, and RMSSD at P5 were observed in pups from mild NEC+sham (N=9), and mild NEC+vagotomy (N=10) groups ($p<0.05$ vs P1 for both groups; Figure 3). Both mild NEC+sham and mild NEC+vagotomy groups had significantly different HF-HRV and RMSSD values as compared to controls at P5 ($p<0.05$ vs control P5 for both groups), but not LF-HRV ($p>0.05$ vs control P5 for both groups).

These data indicate that, when combined with the stress of surgery, NEC attenuates typical developmental increases in HF-HRV power and RMSSD in rat pups at P5.

NEC alters the neurochemical phenotype of myenteric plexus neurons in the jejunum and ileum.

Similar levels of ChAT were observed the myenteric plexus of the corpus, fundus, duodenum, jejunum, and ileum from all groups ($p>0.05$ for all groups vs. control). Data are summarized in Table 2.

Similar levels of nNOS were observed in the myenteric plexus of the corpus, fundus and duodenum, from all groups ($p>0.05$ for all groups vs. control). Conversely, in the myenteric plexus of the jejunum and ileum, similar levels of nNOS were observed in control, control +sham, and control+vagotomy ($p>0.05$ for all groups vs. control), however, there was a significant increase of nNOS in the jejunum and ileum of mild NEC, mild NEC+sham, and mild NEC+vagotomy groups ($p<0.05$ for all groups vs. control). Data are summarized in Table 2 and Figure 4.

These data indicate that NEC alters the postganglionic nitrergic phenotype in the small intestine, but not stomach or duodenum, of NEC rats without altering the cholinergic myenteric phenotype.

Vagotomy in NEC pups increases pro-inflammatory cytokine levels.

At P8/9 similar levels of plasma corticosterone were observed in all groups ($p>0.05$ for all groups vs control; Table 3 and Figure 5).

Similar plasma levels of IFN-γ, IL-10, and TNF-α were measured in all groups ($p>0.05$ for all groups vs. control). Likewise, similar levels of IL-1β and IL-6 were also measured in control, control+sham, control+vagotomy, mild NEC, and mild NEC+sham ($p>0.05$ vs. control) groups. Conversely, elevated levels of IL-1β and IL-6 were observed in mild NEC +vagotomy rats ($p<0.05$ vs. control, mild NEC, and mild NEC+sham). Data are summarized in Table 3 and Figure 5.

These data indicate that there is a significant increase in pro-inflammatory cytokines, but not corticosterone, in the mild NEC+vagotomy group.

DISCUSSION

In the present study we report that an attenuated, established NEC induction model in rat pups i) induced NEC histopathological grade 1–2; ii) altered selectively the neurochemical phenotype of myenteric ganglia in the jejunum and ileum, i.e. the areas affected by NEC pathology; and, when combined with the stress of surgery, iii) reduced the typical developmental increases in HF-HRV power[10,35]. When the attenuated NEC induction was combined with subdiaphragmatic vagotomy, but not sham surgery, the NEC histopathological score was further worsened to grade >2 and there were increases in plasma levels of pro-inflammatory cytokines IL-1β and IL-6, but not corticosterone.

Our evidence is the following. Cold stress and hypoxia are sufficient to induce low grade (mild) NEC in newborn rats, a model for preterm human neonates[23–25], as determined through blinded grading of histology specimens, which showed sloughing of epithelial cells at the tips of villi. Full NEC, including maternal separation and formula feeding in addition to cold stress and hypoxia, resulted in a NEC grade 3–4 phenotype with a high morbidity and 100% mortality rate by P5, instances of pneumatosis intestinalis, and transmural necrosis in the GI tract. In all NEC groups, including mild NEC, i.e. grade 1–2, there was a significant increase in nNOS-, but not ChAT-, immunoreactivity in the distal small intestine.

Our data confirm previous studies that have demonstrated that cold stress and hypoxia are sufficient to induce grade 1–2 NEC in newborn rat pups, which have been shown to be an appropriate and accepted experimental model that reproduces the conditions observed in preterm human neonates[33,36–41]. This mild NEC induction, thus, represents the early phases of the disease, when preventative treatments, such as tighter monitoring of the neonate, increased kangaroo care, receiving mother's own or banked milk, and better antibiotic stewardship, have the most potential for reducing morbidity and mortality. As reported previously[36,37,39], pups induced with fulminant NEC, i.e. maternal separation, hypertonic formula feeding, hypoxia, and cold stress, showed an extreme NEC phenotype with widespread pneumatosis intestinalis, subserosal hemorrhage, extensive areas of necrosis of the GI tract, and 100% mortality rate. These pups were not included in the rest of the study.

These results further indicate that all NEC inductions produced an increase in nNOS immunoreactivity in the distal small intestine, but not in the stomach or the proximal small intestine. These data back the hypothesis that NOS plays a key role in the inflammation that leads to intestinal epithelial cell damage observed in NEC[19,40]. Furthermore, our data would suggest that one of the triggering events, or a consequence, of NEC is, among others, a decrease in gastrointestinal motility possibly due to an increased contribution of the inhibitory non-adrenergic non-cholinergic (NANC) pathway[19]. It has to be kept in mind that, due to technical limitations, the immunohistochemical analysis was conducted in healthy appearing tissue; consequently, the data may be not fully reflective of the changes occurring in damaged tissues. Notably, we did not observe any significant variation of ChAT immunoreactivity in any of the gastrointestinal tissues tested, consistent with previous studies that have shown alterations in NOS in other conditions, such as obesity, ischemia, and diabetes[42–46]

The present results support our previous study in human neonates that showed decreased vagal tone, as measured through HF-HRV, as a prodromal indication of NEC risk in neonates[10]. Conversely, in the same study we reported that neonates who did not develop NEC had a significantly higher HF-HRV power both at the start of the study (day 5–7 of life) as well as at the time other neonates were diagnosed with NEC[10]. The predictive features of HF-HRV were confirmed with the receiver operating characteristic curve, which showed high levels of both sensitivity and specificity of HF-HRV[10]. This observation in neonates, when combined with our present results, confirms HF-HRV as a promising non-invasive predictive method to detect NEC risk before the onset of clinical signs; and supports the predictive use of HF-HRV for both the clinical and laboratory setting in the study of NEC.

Our data show that mild NEC pups have a lesser, albeit significantly different from their own baseline, increase in HF-HRV and RMSSD, which is not observed in mild NEC+sham or mild NEC+vagotomy. Taken together with the increased HF-HRV and RMSSD observed in control+sham, we interpret these data as suggestive that a stressor, such as sham surgery or vagotomy, has profound effects on the already weakened NEC induced pups but does not affect control pups. The similarities between mild NEC+sham and mild NEC+vagotomy are likely due to a "floor" effect on the HF-HRV and RMSSD values. This argument is strengthened by the data showing that in mild NEC pups, but not control, vagotomy worsens both the severity of the histological grading as well as increases the levels of pro inflammatory cytokines, IL-1β and IL-6.

Contrary to the encouraging results obtained with the use of HF-HRV, the present study found that LF-HRV power increases in control, control+sham, and mild NEC pups, but that mild NEC+sham and mild NEC+vagotomy rats are not significantly different from controls at P5. This observation is in line with the not well defined nature of LF-HRV power, in fact some studies claim that it represents the sympathetic response alone, while other studies suggest that it is a hybrid measure of sympathetic and parasympathetic tone[47,48]. Additionally, we report that heart rate increased in all rats between postnatal days one and five, with no significant differences between groups. This trend is consistent with previous observations in rats at early postnatal days, pre-weanling rats typically increase their heart rates between P1 and 10 and then show developmental decreases in the following weeks of life[49,50].

Here we report that subdiaphragmatic unilateral vagotomy increases histological NEC to grade≥2. This histological observation was not likely caused by an increased level of stress since the plasma levels of corticosterone were similar in all groups. Conversely, vagotomy increased the levels of pro-inflammatory cytokines IL-1β and IL-6, similar to what has been observed previously in rodent models of NEC in which the levels of pro-inflammatory cytokines increased with greater NEC severity[36,41]. A similar observation was seen in clinical studies which reported increased blood levels of cytokines, such as IL-1β, IL-6, IL-8, IL-10, and TNF-α, in neonates at advanced NEC stages, i.e. stage 3–4, according to Bell's Modified Staging Criteria[51–54].

The appropriateness of our model of mild NEC and vagotomy as grade≥2 is supported by the observation that we did not measure significant differences in plasma TNF-α levels between control and NEC rats. This is consistent with previous studies showing that TNF-α is involved in systemic inflammation, while NEC is associated with more localized changes within the GI tract[51,52,55–59]. We additionally found no difference in the levels of IFN-γ between groups, most likely due to the role of IFN-γ in viral replication, which is not a part of NEC etiology[52,55–60]. Finally, we report no significant differences in the anti-inflammatory cytokine IL-10 between groups, consistent with our hypothesis that NEC affects pro-inflammatory cytokines such as IL-1β and IL-6[52,53,55–59].

Overall, the present study confirms a preclinical rodent model of NEC as shown through histopathological scoring and altered nitrergic phenotype, and that changes in vagal tone can be detected through HF-HRV in the early phases of the disease, when combined with the

stress of surgery. Furthermore, the addition of a subdiaphragmatic vagotomy worsens the histopathological severity score and increases levels of pro-inflammatory cytokines IL-1β and IL-6. These results confirm that the relationship between NEC and diminished HF-HRV seen in clinical studies can be reproduced in a rodent model. Through the induction of this early point of the disease, we were able to confirm HF-HRV as a promising non-invasive predictive measure to predict NEC risk before the onset of clinical signs, and we propose the further use of HF-HRV in both the clinical and laboratory setting in the study of NEC.

In conclusion, we hypothesize that a combination of reduced vagal tone (as measured by HF-HRV) and increased inhibitory neurotransmitters (NOS-IR) results in a decreased vagal anti-inflammatory effect and an overall reduction of intestinal motility that may contribute to NEC pathology.

ACKNOWLEDGEMENTS

The authors would like to thank Cesare M. & Zoraide Travagli, Leslie & John Meister, and Robert J. & Diane Mitchell for support and encouragement. We also thank Dr. Kirsteen N. Browning for critical comments on the manuscript; Dr. Michelle Titunick, in Dr. Patricia McLaughlin's laboratory, for help with embedding samples in paraffin; and Elizabeth Neely, in Dr. James Connor's laboratory, for help with the corticosterone ELISA assays.

FUNDING & DISCLOSURES

This work was supported by a grant from the National Institutes of Health, USA (NIDDK DK-99350 to RAT and KKD).

KKD & RAT designed the research study; ALM performed all experiments and analyzed the data; ALM, KKD, & RAT wrote the paper.

ABBREVIATIONS

ChAT	choline acetyltransferase
DMV	dorsal motor nucleus of the vagus
ECG	electrocardiogram
GI	gastrointestinal
HF-HRV	high frequency power spectrum of heart rate variability
HRV	heart rate variability
IFN-γ	interferon gamma
IL-1β	interleukin one beta
IL-6	interleukin six
IL-10	interleukin ten
IR	immunoreactivity
LF-HRV	low frequency power spectrum of heart rate variability
NANC	non-adrenergic non-cholinergic vagal pathway

NEC	necrotizing enterocolitis
nNOS	neuronal nitric oxide synthase
PGP	protein gene product 9.5
RMSSD	root mean square of successive differences
Sham	sham vagotomy, i.e. laparotomy
TNF-α	tumor necrosis factor alpha
Vgtx	vagotomy (subdiaphragmatic unilateral)

References

1. Martin JA, Hamilton BE, Osterman MJK, Driscoll AK, Drake P. Births: final data for 2016. Natl Vital Stat Rep. 2018;67(1):1–54.
2. Neu J, Mshvildadze M, Mai V. A roadmap for understanding and preventing necrotizing enterocolitis. Curr Gastroenterol Rep. 2008;10(5):450–457. [PubMed: 18799119]
3. Luig M, Lui K, Nsw, Group AN. Epidemiology of necrotizing enterocolitis--Part II: Risks and susceptibility of premature infants during the surfactant era: a regional study. J Paediatr Child Health. 2005;41(4):174–179. [PubMed: 15813870]
4. Horbar JD, Carpenter JH, Badger GJ, et al. Mortality and Neonatal Morbidity Among Infants 501 to 1500 Grams From 2000 to 2009. Pediatrics. 2012;129(6):1019–1026. [PubMed: 22614775]
5. Shulhan J, Dicken B, Hartling L, Larsen BMK. Current Knowledge of Necrotizing Enterocolitis in Preterm Infants and the Impact of Different Types of Enteral Nutrition Products. Adv Nutr. 2017;8(1):80–91. [PubMed: 28096129]
6. Neu J, Walker WA. Necrotizing enterocolitis. N Engl J Med. 2011;364(3):255–264. [PubMed: 21247316]
7. Jilling T, Lu J, Jackson M, Caplan MS. Intestinal epithelial apoptosis initiates gross bowel necrosis in an experimental rat model of neonatal necrotizing enterocolitis. Pediatr Res. 2004;55(4):622–629. [PubMed: 14764921]
8. Gephart SM, McGrath JM, Effken JA, Halpern MD. Necrotizing enterocolitis risk: state of the science. Adv Neonatal Care. 2012;12(2):77–87; quiz 88–79. [PubMed: 22469959]
9. Nino DF, Sodhi CP, Hackam DJ. Necrotizing enterocolitis: new insights into pathogenesis and mechanisms. Nat Rev Gastroenterol Hepatol. 2016;13(10):590–600. [PubMed: 27534694]
10. Doheny KK, Palmer C, Browning KN, et al. Diminished vagal tone is a predictive biomarker of necrotizing enterocolitis-risk in preterm infants. Neurogastroenterol Motil. 2014;26(6):832–840. [PubMed: 24720579]
11. Rosen H, Craelius W, Curcie D, Hiatt M, Hegyi T. Spectral analysis of heart variability in the newborn infant. Biol Neonate. 2000;77(4):224–229. [PubMed: 10828573]
12. Verklan MT, Padhye NS. Spectral analysis of heart rate variability: an emerging tool for assessing stability during transition to extrauterine life. J Obstet Gynecol Neonatal Nurs. 2004;33(2):256–265.
13. Al-Shargabi T, Reich D, Govindan RB, et al. Changes in Autonomic Tone in Premature Infants Developing Necrotizing Enterocolitis. Am J Perinatol. 2018.
14. Heart rate variability. Standards of measurement, physiological interpretation, and clinical use. Task Force of the European Society of Cardiology and the North American Society of Pacing and Electrophysiology. Eur Heart J. 1996;17(3):354–381. [PubMed: 8737210]
15. Dobrek L, Baranowska A, Thor PJ. Indirect autonomic nervous system activity assessment with heart rate variability in rats with cyclophosphamide-induced hemorrhagic cystitis treated with melatonin or agomelatine. Contemp Oncol (Pozn). 2015;19(5):368–373. [PubMed: 26793020]

16. Goncalves H, Henriques-Coelho T, Bernardes J, Rocha AP, Brandao-Nogueira A, Leite-Moreira A. Analysis of heart rate variability in a rat model of induced pulmonary hypertension. Med Eng Phys. 2010;32(7):746–752. [PubMed: 20547091]
17. Porges SW. Vagal tone: a physiologic marker of stress vulnerability. Pediatrics. 1992;90(3 Pt 2): 498–504. [PubMed: 1513615]
18. Porges SW. Cardiac vagal tone: a physiological index of stress. Neurosci Biobehav Rev. 1995;19(2):225–233. [PubMed: 7630578]
19. Travagli RA, Anselmi L. Vagal neurocircuitry and its influence on gastric motility. Nat Rev Gastroenterol Hepatol. 2016;13(7):389–401. [PubMed: 27251213]
20. Stone ML, Tatum PM, Weitkamp JH, et al. Abnormal heart rate characteristics before clinical diagnosis of necrotizing enterocolitis. Journal of perinatology : official journal of the California Perinatal Association. 2013.
21. Vandenbroucke L, Doyen M, Le Lous M, et al. Chorioamnionitis following preterm premature rupture of membranes and fetal heart rate variability. PLoS One. 2017;12(9):e0184924. [PubMed: 28945767]
22. Garzoni L, Faure C, Frasch MG. Fetal cholinergic anti-inflammatory pathway and necrotizing enterocolitis: the brain-gut connection begins in utero. Front Integr Neurosci. 2013;7:57. [PubMed: 23964209]
23. Romijn HJ, Hofman MA, Gramsbergen A. At What Age Is the Developing Cerebral-Cortex of the Rat Comparable to That of the Full-Term Newborn Human Baby. Early Human Development. 1991;26(1):61–67. [PubMed: 1914989]
24. Bayer SA, Altman J, Russo RJ, Zhang X. Timetables of neurogenesis in the human brain based on experimentally determined patterns in the rat. Neurotoxicology. 1993;14(1):83–144. [PubMed: 8361683]
25. Clancy B, Darlington RB, Finlay BL. Translating developmental time across mammalian species. Neuroscience. 2001;105(1):7–17. [PubMed: 11483296]
26. Underwood MA, Kananurak A, Coursodon CF, et al. Bifidobacterium bifidum in a rat model of necrotizing enterocolitis: antimicrobial peptide and protein responses. Pediatr Res. 2012;71(5): 546–551. [PubMed: 22322385]
27. Lu P, Sodhi CP, Jia H, et al. Animal models of gastrointestinal and liver diseases. Animal models of necrotizing enterocolitis: pathophysiology, translational relevance, and challenges. Am J Physiol Gastrointest Liver Physiol. 2014;306(11):G917–G928. [PubMed: 24763555]
28. The Neu J. 'myth' of asphyxia and hypoxia-ischemia as primary causes of necrotizing enterocolitis. Biol Neonate. 2005;87(2):97–98. [PubMed: 15528876]
29. Browning KN, Babic T, Holmes GM, Swartz EM, Travagli RA. A critical re-evaluation of the specificity of action of perivagal capsaicin. J Physiol. 2013;591(6):1563–1580. [PubMed: 23297311]
30. Ramshur JT. DESIGN, EVALUATION, AND APPLICAION OF HEART RATE VARIABILITY ANALYSIS SOFTWARE (HRVAS), The University of Memphis; 2010.
31. Kuwahara M, Yayou K, Ishii KJ, Hashimoto S, Tsubone H, Sugano S. Power Spectral-Analysis of Heart-Rate-Variability as a New Method for Assessing Autonomic Activity in the Rat. J Electrocardiol. 1994;27(4):333–337. [PubMed: 7815012]
32. Aubert AE, Ramaekers D, Beckers F, et al. The analysis of heart rate variability in unrestrained rats. Validation of method and results. Comput Methods Programs Biomed. 1999;60(3):197–213. [PubMed: 10579513]
33. Jilling T, Lu J, Jackson M, Caplan MS. Intestinal epithelial apoptosis initiates gross bowel necrosis in an experimental rat model of neonatal necrotizing enterocolitis. Pediatr Res. 2004;55(4):622–629. [PubMed: 14764921]
34. Guo JJ, Browning KN, Rogers RC, Travagli RA. Catecholaminergic neurons in rat dorsal motor nucleus of vagus project selectively to gastric corpus. AJPgastro. 2001;280:G361–G367.
35. Doheny KK, Tang XR, Browning KN, Palmer C, Travagli RA. Correlation Between Decreased Vagal Activity and Necrotizing Enterocolitis (NEC). Gastroenterology. 2012;142(5):S47–S48.

36. Dvorak B, Halpern MD, Holubec H, et al. Maternal milk reduces severity of necrotizing enterocolitis and increases intestinal IL-10 in a neonatal rat model. Pediatric Research. 2003;53(3): 426–433. [PubMed: 12595590]
37. Dvorak B, Halpern MD, Holubec H, et al. Epidermal growth factor reduces the development of necrotizing enterocolitis in a neonatal rat model. Am J Physiol-Gastr L. 2002;282(1):G156–G164.
38. Dingle BM, Liu Y, Fatheree NY, Min J, Rhoads JM, Tran DQ. FoxP3(+) regulatory T cells attenuate experimental necrotizing enterocolitis. PLoS One. 2013;8(12):e82963. [PubMed: 24367573]
39. Tian R, Liu SX, Williams C, et al. Characterization of a necrotizing enterocolitis model in newborn mice. Int J Clin Exp Med. 2010;3(4):293–302. [PubMed: 21072263]
40. Grishin A, Bowling J, Bell B, Wang J, Ford HR. Roles of nitric oxide and intestinal microbiota in the pathogenesis of necrotizing enterocolitis. J Pediatr Surg. 2016;51(1):13–17. [PubMed: 26577908]
41. Rentea RM, Welak SR, Fredrich K, et al. Early enteral stressors in newborns increase inflammatory cytokine expression in a neonatal necrotizing enterocolitis rat model. Eur J Pediatr Surg. 2013;23(1):39–47. [PubMed: 23165517]
42. Shah V, Lyford G, Gores G, Farrugia G. Nitric oxide in gastrointestinal health and disease. Gastroenterology. 2004;126(3):903–913. [PubMed: 14988844]
43. Stenkamp-Strahm CM, Nyavor YE, Kappmeyer AJ, Horton S, Gericke M, Balemba OB. Prolonged high fat diet ingestion, obesity, and type 2 diabetes symptoms correlate with phenotypic plasticity in myenteric neurons and nerve damage in the mouse duodenum. Cell Tissue Res. 2015;361(2): 411–426. [PubMed: 25722087]
44. Yarandi SS, Srinivasan S. Diabetic gastrointestinal motility disorders and the role of enteric nervous system: current status and future directions. Neurogastroenterol Motil. 2014;26(5):611–624. [PubMed: 24661628]
45. Rivera LR, Thacker M, Castelucci P, Bron R, Furness JB. The reactions of specific neuron types to intestinal ischemia in the guinea pig enteric nervous system. Acta Neuropathol. 2009;118(2):261–270. [PubMed: 19466432]
46. de Vries P, Soret R, Suply E, Heloury Y, Neunlist M. Postnatal development of myenteric neurochemical phenotype and impact on neuromuscular transmission in the rat colon. Am J Physiol Gastrointest Liver Physiol. 2010;299(2):G539–547. [PubMed: 20522637]
47. Rowan WH, Campen MJ, Wichers LB, Watkinson WP. Heart rate variability in rodents: uses and caveats in toxicological studies. Cardiovasc Toxicol. 2007;7(1):28–51. [PubMed: 17646680]
48. Laborde S, Mosley E, Thayer JF. Heart Rate Variability and Cardiac Vagal Tone in Psychophysiological Research - Recommendations for Experiment Planning, Data Analysis, and Data Reporting. Front Psychol. 2017;8:213. [PubMed: 28265249]
49. Quigley KS, Shair HN, Myers MM. Parasympathetic control of heart period during early postnatal development in the rat. J Auton Nerv Syst. 1996;59(1–2):75–82. [PubMed: 8816368]
50. Hofer MA, Reiser MF. The development of cardiac rate regulation in preweanling rats. Psychosom Med. 1969;31(5):372–388. [PubMed: 5350296]
51. Bhatia AM, Stoll BJ, Cismowski MJ, Hamrick SE. Cytokine levels in the preterm infant with neonatal intestinal injury. Am J Perinatol. 2014;31(6):489–496. [PubMed: 23966125]
52. Benkoe T, Baumann S, Weninger M, et al. Comprehensive evaluation of 11 cytokines in premature infants with surgical necrotizing enterocolitis. PLoS One. 2013;8(3):e58720. [PubMed: 23472217]
53. Maheshwari A, Schelonka RL, Dimmitt RA, et al. Cytokines associated with necrotizing enterocolitis in extremely-low-birth-weight infants. Pediatr Res. 2014;76(1):100–108. [PubMed: 24732104]
54. Bell MJ, Ternberg JL, Feigin RD, et al. Neonatal necrotizing enterocolitis. Therapeutic decisions based upon clinical staging. Ann Surg. 1978;187(1):1–7. [PubMed: 413500]
55. Chavez Valdez R, Ahlawat R, Wills-Karp M, Nathan A, Ezell T, Gauda EB. Correlation between serum caffeine levels and changes in cytokine profile in a cohort of preterm infants. J Pediatr. 2011;158(1):57–64, 64 e51. [PubMed: 20691455]

56. Al-Shargabi T, Govindan RB, Dave R, et al. Inflammatory cytokine response and reduced heart rate variability in newborns with hypoxic-ischemic encephalopathy. Journal of perinatology : official journal of the California Perinatal Association. 2017;37(6):668–672. [PubMed: 28252659]

57. Lusyati S, Hulzebos CV, Zandvoort J, Sauer PJ. Levels of 25 cytokines in the first seven days of life in newborn infants. BMC research notes. 2013;6:547. [PubMed: 24359685]

58. Kleiner G, Marcuzzi A, Zanin V, Monasta L, Zauli G. Cytokine levels in the serum of healthy subjects. Mediators of inflammation. 2013;2013:434010. [PubMed: 23533306]

59. Bennet SMP, Polster A, Tornblom H, et al. Global Cytokine Profiles and Association With Clinical Characteristics in Patients With Irritable Bowel Syndrome. Am J Gastroenterol. 2016;111(8): 1165–1176. [PubMed: 27272011]

60. Maheshwari A, Schelonka RL, Dimmitt RA, et al. Cytokines associated with necrotizing enterocolitis in extremely-low-birth-weight infants. Pediatr Res. 2014;76(1):100–108. [PubMed: 24732104]

KEY POINTS

- Non-invasive tests predicting necrotizing enterocolitis (NEC) onset are needed. We have shown previously the high-frequency spectrum of heart rate variability (HF-HRV) may be such a predictive test.
- Mild NEC induction and laparotomy/vagotomy in rat pups attenuates developmental increases in HF-HRV and increases nitrergic-immunoreactivity in the myenteric plexus of the distal small intestine. Subdiaphragmatic vagotomy worsens NEC histopathology and increases plasma pro-inflammatory cytokines.
- HF-HRV shows promise as a non-invasive predictive test to assess NEC risk in both experimental and clinical settings.

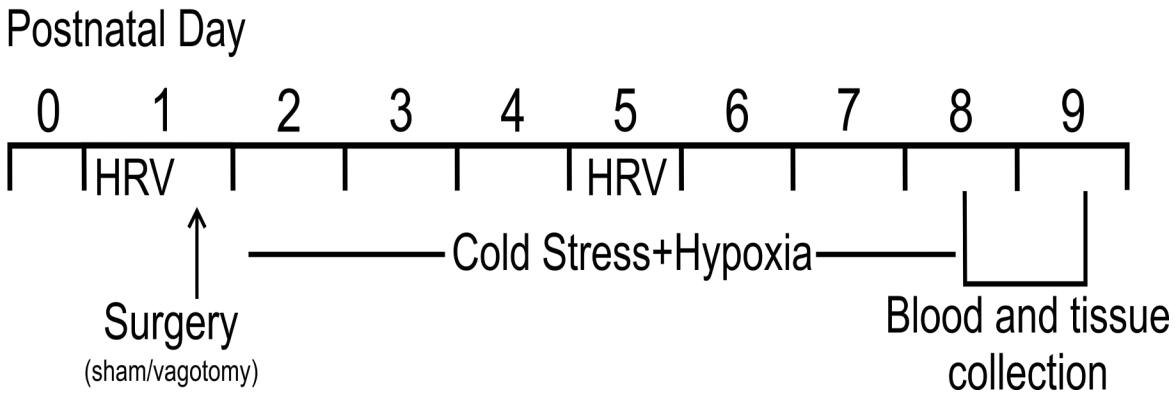

Figure 1. Experimental design.
Schematic workflow diagram of the experimental design.

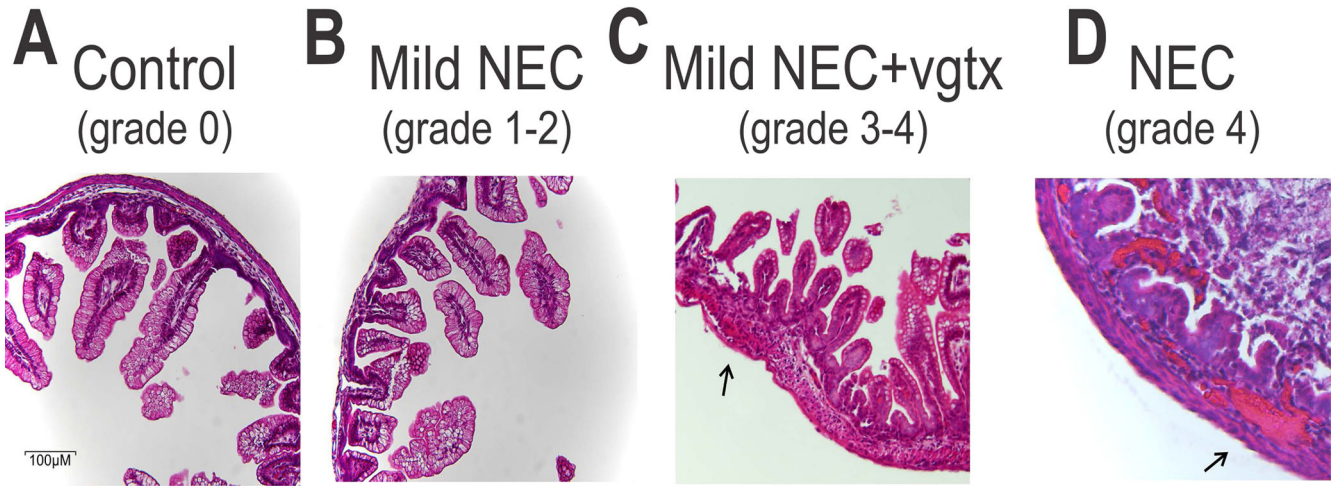

Figure 2. Histological grading of NEC.

Representative micrographs (20x magnification) showing H&E stained sections of ileum from control (panel A), mild NEC (B), mild NEC+vagotomy (vgtx; C), and NEC (D) pups. Mild NEC induced sloughing of epithelial cells at the tips of the villi, while vagotomy worsened the histopathological profile to include mid-villous necrosis. Note the subserosal hemorrhage (arrows) in the more severe grades of NEC.

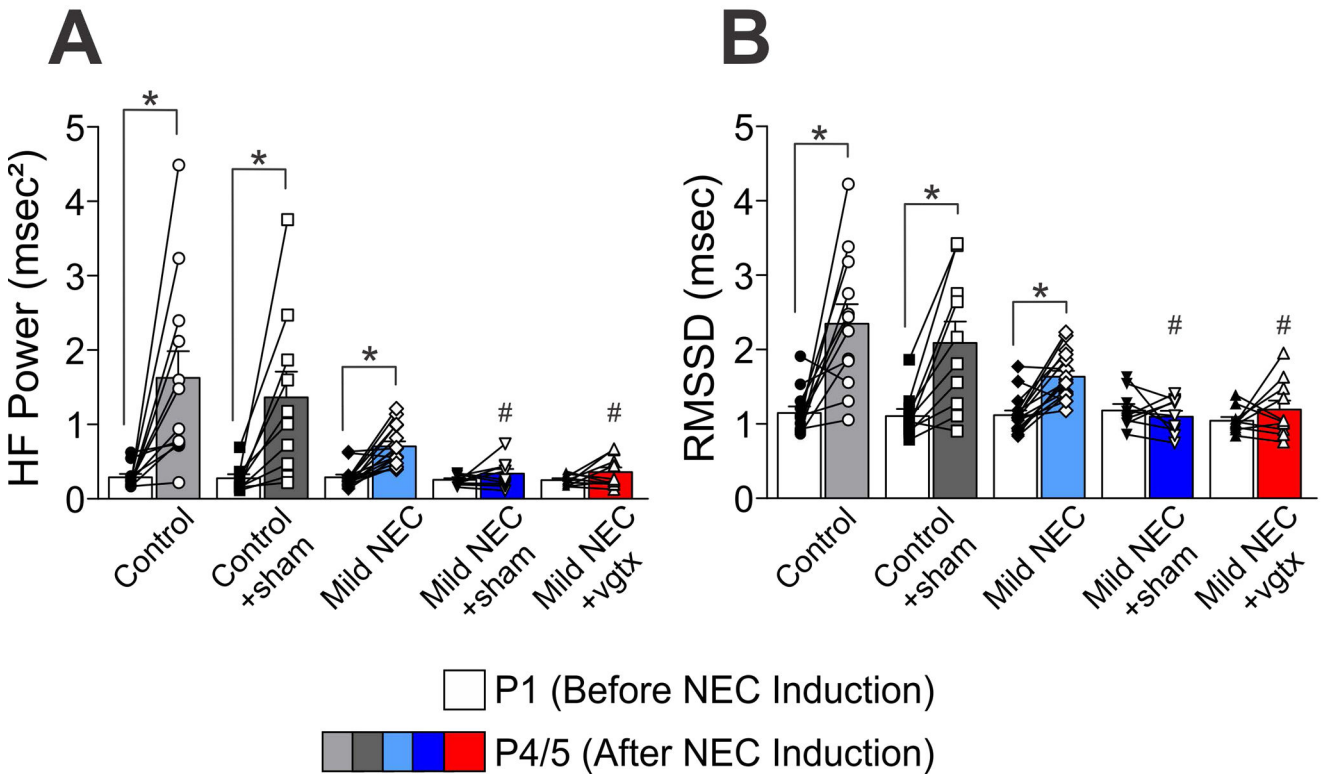

Figure 3. NEC attenuates developmental HRV increases.

Graphic summary of HF-HRV (panel A) and RMSSD (B) results showing that at postnatal day 1 (P1), all groups have similar levels, however, only control, control+sham, and mild NEC groups showed increased values at postnatal day 4/5 (P4/5; *$p<0.05$ P1 vs P4/5). Mild NEC+sham and mild NEC+vagotomy (vgtx) values at P4/5 are significantly lower than controls at the same time point ($^{\#}p<0.05$ vs Control P4/5).

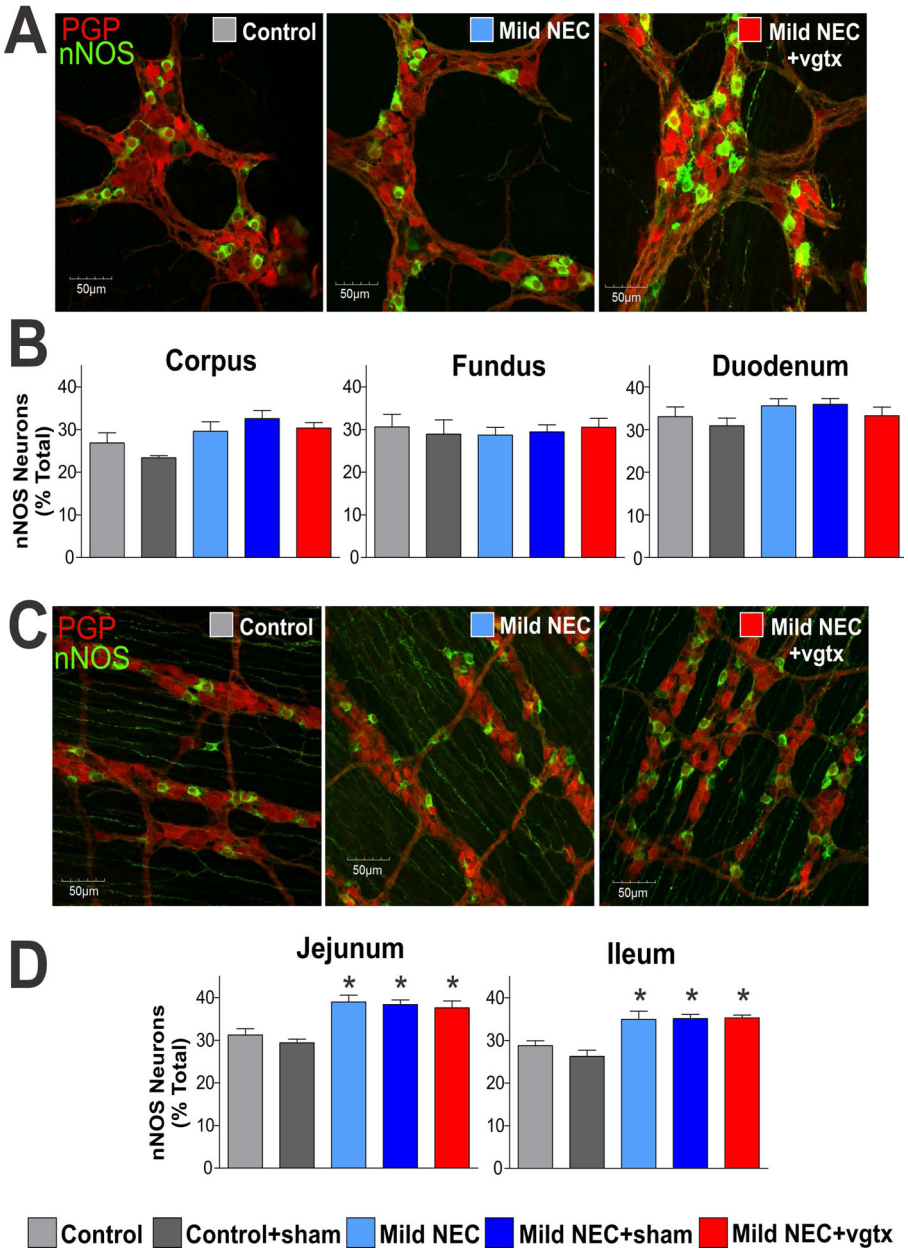

Figure 4. NEC induction alters the neurochemical phenotype of myenteric plexus neurons in the jejunum and ileum.

A) Representative micrographs (40x magnification) depicting myenteric ganglia of the corpus. B) Summary graphs showing that similar levels of nNOS were observed in the myenteric plexus of the corpus, fundus, and duodenum of all groups. C) Representative micrographs (40x magnification) depicting myenteric ganglia of the ileum. D) Summary graphs showing the increase in nNOS-immunoreactivity in the myenteric plexus of the jejunum and ileum of mild NEC, mild NEC+sham, and mild NEC+vagotomy (vgtx) groups (*$p<0.05$ vs control and control+sham).

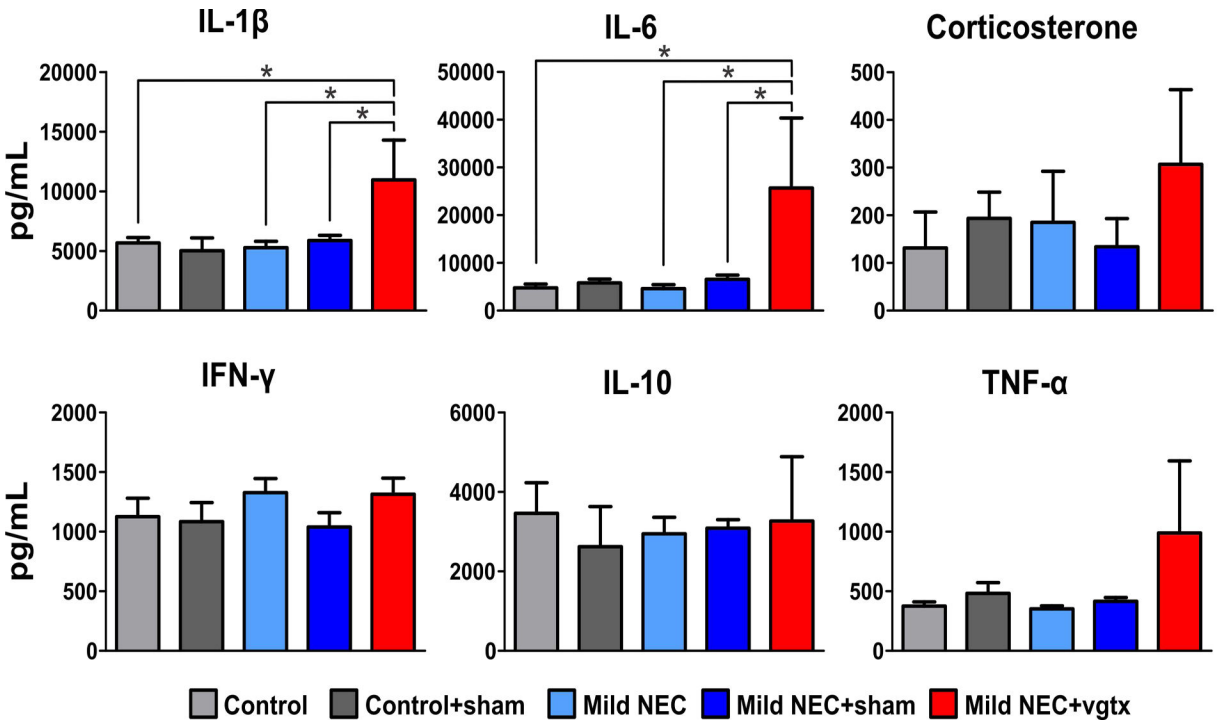

Figure 5. NEC increases pro-inflammatory cytokine levels.

Summary graphic showing the increase in plasma IL-1β and IL-6 levels in mild NEC +vagotomy rats, indicating a significant increase in pro-inflammatory cytokines (*$p<0.05$ vs control, mild NEC, and mild NEC+sham).

Table 1.

Summary of heart variability data (data presented as mean±SEM).

	Heart Rate (beats min^{-1})		HF-Power (ms^2)		LF-Power (ms^2)		RMSSD (ms)	
	P1	**P4/5**	**P1**	**P4/5**	**P1**	**P4/5**	**P1**	**P4/5**
Control (n=12)	301.4±6.0	350.8±9.8 *	0.29±0.04	1.63±0.36 *	0.10±0.03	0.64±0.21 *	1.15±0.09	2.35±0.26 *
Control +sham (n=10)	256.2±6.4	323.6±6.7 *	0.28±0.06	1.36±0.35 *	0.08±0.02	1.11±0.35 *	1.11±0.10	2.09±0.29 *
Control +vagotomy (n=6)	286.9±13.2	350.9±15.0 *	0.31±0.10	2.36±1.02	0.10±0.03	1.33±0.83	1.18±0.19	2.33±0.63
Mild NEC (n=16)	296.6±8.6	341.2±5.8 *	0.29±0.04	0.71±0.06 *	0.09±0.02	0.23±0.04 *	1.12±0.06	1.63±0.08 *
Mild NEC +sham (n=9)	284.7±11.1	350.5±6.1 *	0.26±0.02	0.34±0.06 #	0.05±0.01	0.11±0.03	1.18±0.08	1.10±0.08 #
Mild NEC +vagotomy (n=10)	302.0±9.0	364.8±7.0 *	0.25±0.02	0.36±0.06 #	0.07±0.01	0.15±0.06	1.04±0.05	1.19±0.12 #

* $p<0.05$ vs P1

# $p<0.05$ vs control at same time point

Table 2.

Summary of choline acetyl transferase (ChAT) immunohistochemistry data (data presented as mean±SEM).

	Corpus		Fundus		Duodenum		Jejunum		Ileum	
	ChAT	***nNOS***	***ChAT***	***nNOS***	***ChAT***	***nNOS***	***ChAT***	***nNOS***	***ChAT***	***nNOS***
Control (n=6–10)	6.3±0.7	26.9±2.4	7.3±1.3	30.6±3.0	5.6±0.5	33.0±2.3	5.4±0.4	31.2±1.5	7.8±0.8	28.8±1.2
Control+ sham (n=6–7)	4.8±0.5	23.4±0.5	5.6±0.9	30.1±2.8	4.9±0.3	30.9±1.8	5.2±0.2	29.4±0.9	7.3±1.7	25.2±1.6
Control+ vagotomy (n=5)	6.9±0.5	25.0±0.3	6.7±0.3	23.9±1.0	6.4±0.2	25.4±0.8	6.1±0.2	26.1±0.5	6.2±0.3	25.2±0.7
Mild NEC (n=6–11)	5.9±0.5	29.6±2.2	6.9±1.2	28.7±1.8	6.0±0.3	35.6±1.7	5.4±0.2	38.9±1.6*	6.2±0.8	34.9±1.9*
Mild NEC+ sham (n=6–13)	5.6±0.4	32.6±1.9	6.2±0.3	29.4±1.7	5.2±0.2	35.9±1.3	5.8±0.5	38.4±1.1*	7.4±0.7	35.1±1.0*
Mild NEC+ vagotomy (n=6–8)	6.8±0.9	30.4±1.3	6.7±0.8	30.6±2.1	6.3±0.6	33.3±2.0	6.5±0.6	37.6±1.6*	6.9±0.8	35.3±0.7*

*p<0.05 vs. control in same tissue type and stain

Table 3.

Summary of plasma corticosterone and cytokine level data (data presented as mean±SEM).

	Cort (pg mL^{-1})	Cytokine Level (pg mL^{-1})				
		IL-6	IL-1β	IL-10	IFN-γ	TNF-α
Control	132±75 (n=10)	4759±788 (n=9)	5674±445 (n=10)	3463±770 (n=6)	1125±156 (n=8)	376±35 (n=8)
Control +sham	193±55 (n=6)	5814±770 (n=3)	5970±906 (n=6)	2624±1009 (n=4)	1085±160 (n=4)	482±90 (n=6)
Control +vgtx	236±187 (n=3)	12422±1973 (n=3)	9142±331 (n=3)	7543±3626 (n=4)	1554±300 (n=4)	954±56 (n=4)
Mild NEC	185±107 (n=14)	4597±846 (n=9)	5275±526 (n=12)	2948±416 (n=4)	1328±118 (n=12)	352±26 (n=10)
Mild NEC +sham	134±59 (n=12)	6548±875 (n=12)	5871±438 (n=13)	3088±217 (n=9)	1039±121 (n=13)	416±33 (n=12)
Mild NEC +vgtx	307±157 (n=10)	25698±14640 * (n=5)	10964±3323 * (n=6)	3269±1619 (n=8)	1313±136 (n=8)	989±605 (n=8)

* $p<0.05$ vs. control, mild NEC, and mild NEC+sham